Behavior of Boron in Molten Aluminum and its Grain Refinement Mechanism

HOUSHANG D. ALAMDARI, DOMINIQUE DUBÉ, and PASCAL TESSIER

The mechanism of heterogeneous grain refining of aluminum by ultrafine elemental boron particles was investigated. In order to facilitate the observation of the boron-aluminum interface, a boron filament was introduced in a melt at 1013 K (740 °C) containing different levels of Ti. The Al/B interface was studied using transmission electron microscopy and different phases were identified using the electron diffraction method. The experimental results showed that boron is dissolved in pure aluminum while its dissolution is inhibited in presence of titanium solute. A thin layer of TiB_2 formed at the surface of boron thickens with residence time in the melt. The mechanisms by which aluminum is crystallized on boron are discussed.

I. INTRODUCTION

THE addition of grain refiners into molten aluminum alloys is a common industrial practice to suppress the growth of columnar grains, to promote the formation of fine grains, and to improve castability and product quality. Grain refiners are usually added as Al-based master alloys that are rich in at least one of the following elements: titanium, boron and carbon. There are several types of grain refiners. Those produced by reaction of molten aluminum with halide salts (K_2TiF_6 and KBF_4) and containing 5 pct Ti and 1 pct B, are the most widely used by industry. Their typical microstructure consists of TiB_2 particles, $TiAl_3$ needles and Ti solute in an aluminum matrix. Small additions of such master alloys in aluminum alloys (usually at 0.01 pct Ti and 0.002 pct B levels) result in a fine and equiaxed solidification microstructure. An appropriate temperature of addition practically lies between the liquids and 1073 K (800 °C).

A great deal of fundamental research has been done over the past 50 years in order to understand the possible mechanisms by which grain refiners yield a fine microstructure. The majority of fundamental research works have focused on the refining mechanisms of Al-Ti-B master alloys and several theories have been postulated in this matter which were summarized in very useful comprehensive reviews.[1–4] According to these theories, the refinement effect could be ascribed to two phenomena: (i) the growth restriction factor and (ii) the inoculation and heterogeneous nucleation. The growth restriction is explained by the diffusion of solute atoms at the liquid/solid interface. In the inoculation theory, however, α-Al grains grow on the nucleation sites that are introduced in the liquid metal by the master alloy. Small particles of $TiAl_3$, $(Ti-Al)B_2$, and TiB_2[5–9] have been proposed as potential nuclei contributing to the formation of α-Al and the efficiency and stability of these particles have been extensively studied. According to a general consensus, the heterogeneous nucleation of aluminum is attributed to the presence of TiB_2 particles when an Al-Ti-B refiner is used. Some experimental evidence confirmed the nucleation potential of TiB_2 particles, while it was also shown that TiB_2 could be surrounded by a thin layer of $TiAl_3$ phase which acts as the nucleation site.[10–15]

Although the efficiency of grain refiners has been improved considerably over the past decades, there are still several issues which need to be addressed. One of these issues is the difficulty of controlling the size, morphology and agglomeration of TiB_2 particles in Al-Ti-B master alloy. Individual particles of TiB_2 have typically a size between 0.5 and 2 μm but some reach 10 μm. Agglomeration of particles increases with increasing residence time in the melt and worsens in the presence of halide salt traces[16,17] although recent studies have shown that Mg additions reduce the agglomeration and increase nucleation efficiency in Al-Si alloys.[18] The coarse TiB_2 particles and agglomerates are a serious concern and can cause surface defects, especially if the aluminum is to be rolled in thin foils. Settling of TiB_2 particles is another issue. These particles tend to settle at the bottom of crucibles resulting in the formation of sludge and reducing the overall efficiency of the refiner. Grain refining of recycled aluminum is also a growing concern in cast houses. The level of Ti must be kept under the peritectic concentration in order to prevent the formation of brittle $TiAl_3$ needles during solidification. Recycled metals contain a considerable amount of titanium. Addition of Ti-containing refiners in a recycled metal causes an increase of Ti level and limits the use of recycled metals in melt charge. Foundries keep this level typically under 1000 ppm. Titanium level is controlled

HOUSHANG D. ALAMDARI and DOMINIQUE DUBÉ, Professors, are with the Department of Mining, Metallurgical and Materials Engineering, Laval University, Quebec, QC, G1K 7P4, Canada. Contact e-mail: Houshang.alamdari@gmn.ulaval.ca PASCAL TESSIER, Senior Research Scientist, is with Air Liquide Research and Development, Delaware Research and Technology Center, 200 GBC Drive, Newark, DE, 19702.
Manuscript submitted February 7, 2012.
Article published online September 13, 2012.

by mixing recycled and pure aluminum in the melt charge.

In an attempt to overcome some of the abovementioned issues, Alamdari et al.[19] have proposed a novel process for grain refinement of aluminum alloys by using fine elemental boron particles. These grain refiners are in the form of Al-matrix composites in which elemental boron particles are finely dispersed using high energy ball milling. The grain refining tests revealed that the addition of boron alone at the level of 0.002 pct does not provide any grain refining effect in pure aluminum. However they showed that when titanium is introduced prior to or along with boron this refiner is more efficient than the conventional Al-5Ti-1B refiners for commercially pure aluminum and some Al-Si based alloys such as A356 and A357. These observations confirm the fact that boron particles do not survive in pure aluminum above 1013 K (740 °C). However, in the presence of Ti, boron particles are not only protected in the melt but also contribute efficiently to heterogeneous nucleation of aluminum. Beside its great efficiency and good control of particle size refining, this grain refiner may also offer the possibility of treating recycled aluminum without any titanium addition. The mechanism by which elemental boron particles act as potential nuclei is however still unknown.

The purpose of this paper is to study the behavior of elemental boron in liquid aluminum in order to elucidate its influence on the grain refining mechanism of boron particles. The boron filament was introduced into liquid aluminum containing different concentrations of dissolved titanium and the microstructure and composition at the boron/aluminum interface were studied. The boron fiber facilitates the study of the boron-aluminum interface after immersion in liquid aluminum.

II. EXPERIMENTAL DETAILS

A series of aluminum melts with titanium levels varying between 20 and 500 ppm were prepared in an alumina crucible using an electric furnace heated at 1013 K (740 °C). The chemical composition of the pure aluminum used to prepare the melts is given in Table I. For each sample, approximately 200 g of alloy was melted.

The titanium level in the melt was adjusted by adding a master alloy containing 6 wt pct Ti. The master alloy had been previously prepared in the laboratory by dissolving 6 wt pct pure titanium powder in pure molten aluminum. The required mass of master alloy was added to molten aluminum at 1053 K (780 °C) prior to stirring and reducing the temperature to 1013 K (740 °C).

A boron filament (supplied by Specialty Materials Inc., USA) was then introduced into both pure aluminum and Al-Ti melts. Figure 1 shows the surface aspect of the

boron filament and reveals its polycrystalline structure. The filament is composed of a tungsten wire of 10 μm diameter coated with 70 μm thick high purity boron.

In a first series of experiments, boron filaments were immersed into pure aluminum and Al-Ti melts for different periods of time varying between 5 and 15 minutes. In order to provide Al-Ti melts, titanium was added to the melt 30 minutes before introducing the boron filament. The crucible was then taken out of the furnace and allowed to cool rapidly. Duration of solidification was about one minute. The solidified samples were then cut and polished and the cross section of the filament was characterized using optical and scanning electron microscopy in order to reveal the boron-aluminum interface.

In a second series of experiments, two specimens were immersed into the melt for 30 minutes and 6 hours respectively and then rapidly pulled out of the melt in order to allow rapid quenching directly from the melt temperature. This second series of test was performed to eliminate any cooling artifact at the interface and to reveal the interface state as it was in the melt. The specimens were thinned using focused ion beam (FIB) and their interface was examined using a transmission electron microscope (TEM).

III. RESULTS AND DISCUSSION

A. Stability of Elemental Boron in Pure Al and Al-Ti Melts

Figure 2 shows the polished cross-section of a boron fiber after immersion in pure aluminum melt for 5 minutes and solidification. The fiber remained in crucible during solidification (solidification time was about 1 minutes). Figure 3 shows the cross section of a second filament immersed 12 minutes and solidified in identical conditions. As seen, the boron filament dissolves rapidly in pure aluminum melt so that after 12 minutes its diameter was reduced from 150 to 50 μm. After 15 minutes, the boron filament was completely dissolved in aluminum. These observations confirms that fine boron particles would dissolve very rapidly in pure aluminum at 1013 K (740 °C) and consequently they do not contribute to the heterogeneous nucleation of aluminum.

Since the grain refining effect of boron particles had been reported in a melt containing at least 100 ppm Ti,[19] the stability of a boron filament in melts having different concentrations of titanium was also investigated in order to reveal the effect of Ti on boron dissolution rate. Titanium was added to the melt 30 minutes before introducing the boron filament, providing melts containing between 50 and 500 ppm Ti. Figure 4 shows the polished cross section of the

Table I. Chemical Composition of the Liquid Aluminum Bath

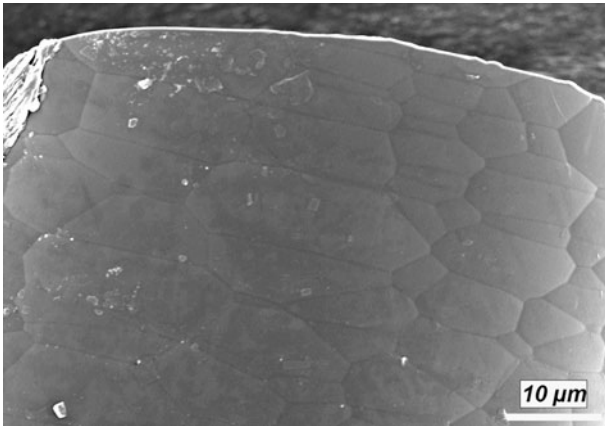| Element	Al	Si	Fe	Cu	Zn	V	Pb	Ti
Wt pct	99.995	0.001	0.0009	0.0009	<0.0001	<0.0001	<0.0001	<0.0020

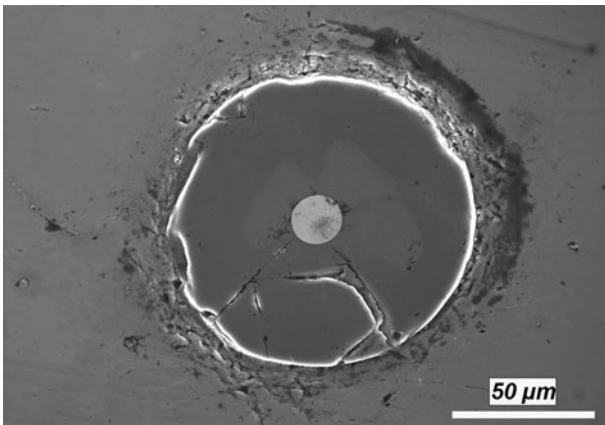Fig. 1—SEM image of the boron filament surface.

Fig. 2—Cross-section of a boron fiber that was immersed for 5 min in pure molten aluminum at 1013 K (740 °C). The fiber remained in the melt during solidification. The tungsten wire is visible at the center.
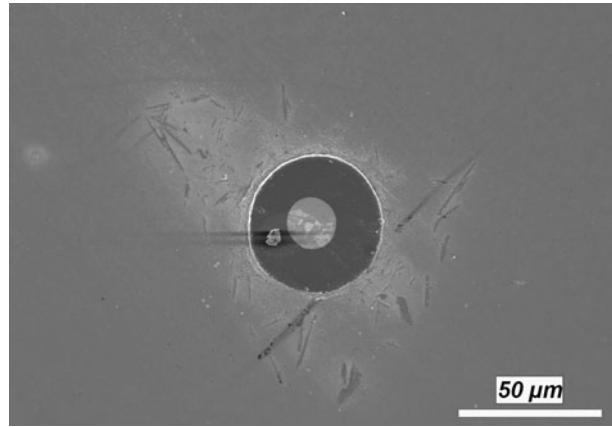

Fig. 3—Cross-section of a boron fiber that was immersed for 12 min in pure molten aluminum at 1013 K (740 °C). The fiber remained in the melt during solidification.
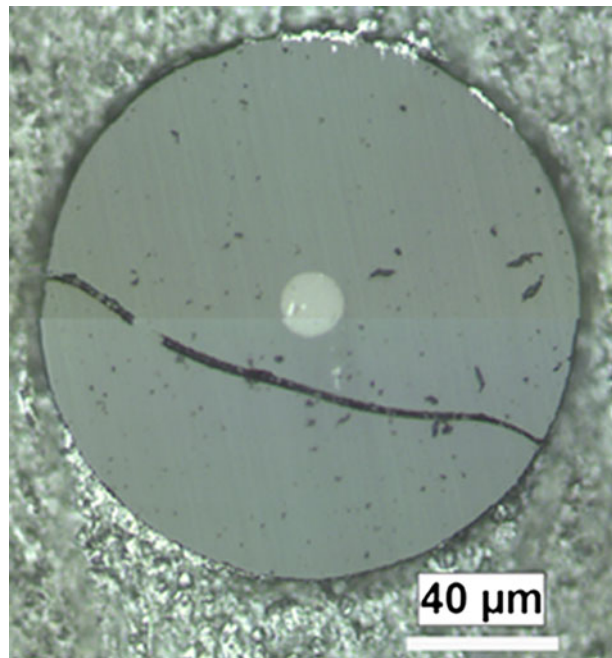

Fig. 4—Cross-section of a boron fiber after 10 min of immersion in molten aluminum containing 500 ppm Ti at 1013 K (740 °C). The fiber remained in the melt during solidification.

boron filament after being kept for 10 minutes in an aluminum melt containing 500 ppm Ti. The fiber remained in the melt during solidification. A similar behavior was observed in melts containing 100, 200 and 500 ppm Ti. This concentration of titanium is typically found in cast industrial alloys. The diameter of the boron filament remains unchanged indicating that this concentration of titanium solute prevents the dissolution of boron in the melt. Even after 6 hours in the melt, the filament kept its initial diameter. The same experiments conducted with lower Ti levels revealed that the amount of Ti required for protection of boron wire is as low as 150 ppm. These observations confirm that the dissolved titanium efficiently stabilizes boron particles in an aluminum melt where they could eventually contribute to heterogeneous nucleation.

B. Boron/Aluminum Interface

The interface of the boron filament and aluminum matrix was examined after different immersion times in order to understand the mechanisms by which boron is protected in the presence of titanium. First, a boron filament was introduced into an aluminum melt containing 500 ppm Ti at 1013 K (740 °C), maintained in the melt for 15 minutes and then rapidly withdrawn. Figure 5 shows a TEM image of the filament/aluminum interface and Figure 6 illustrates the elemental line scan across this interface following the a-b path. Aluminum was detected in the boron filament indicating that it diffuses rapidly within boron. A strong peak of oxygen was also detected at the interface. The source of oxygen could be an oxide skin entrained from the melt surface or oxygen at the surface of the boron filament, usually in the form of boron oxide, most likely combined as aluminum oxide after immersion. A very weak peak of titanium was also detected at the interface after long counting times. The massive phase formed in front of the interface was
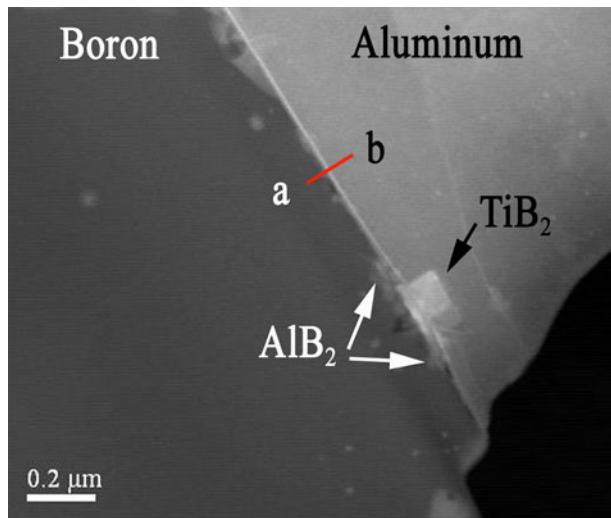
Fig. 5—Boron-aluminum interface with the reaction interlayer revealing the formation of AlB_2 and TiB_2 phases. The fiber was immersed in aluminum melt containing 500 ppm Ti for 15 min at 1013 K (740 °C) and rapidly withdrawn.
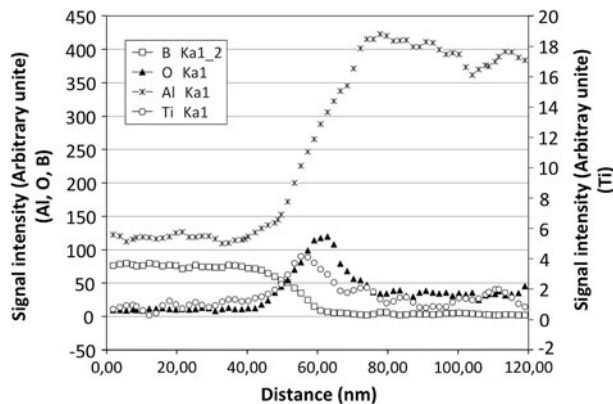

Fig. 6—Elemental profile across the boron-aluminum interface along the a-b path shown in Fig. 5. The concentrations of aluminum, boron, and oxygen are read on the left axis and that of titanium on the right one.

identified as TiB_2 using electron diffraction. The gray zones just behind the interface were identified as AlB_2.

The interface was also examined after immersion in the melt for 6 hours following the same procedure. Figure 7 shows a dark field TEM image of the interface. Compared to the interface after 15 minutes of immersion (Figure 5), 6 hours of immersion results in a continuous layer of TiB_2 blocky crystals in front of the interface while the gray AlB_2 zone behind the interface was thickened (Figure 7). Figure 8a shows the electron diffraction pattern obtained in the gray zone behind the interface (inside boron filament) and corresponds to AlB_2 structure. The electron diffraction pattern shown in Figure 8b were obtained in the blocky crystals in front of the interface and corresponds to TiB_2. Variations in the thickness of AlB_2 zone indicate that the rate of diffusion of Al in boron is not the same along the interface. This could be attributed to surface defects and asperities on the boron filament.
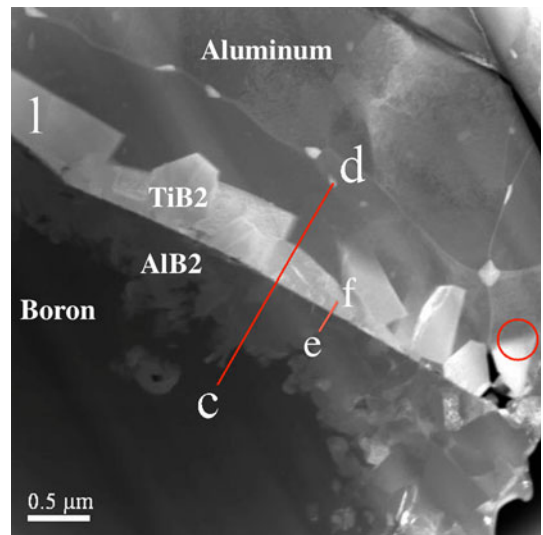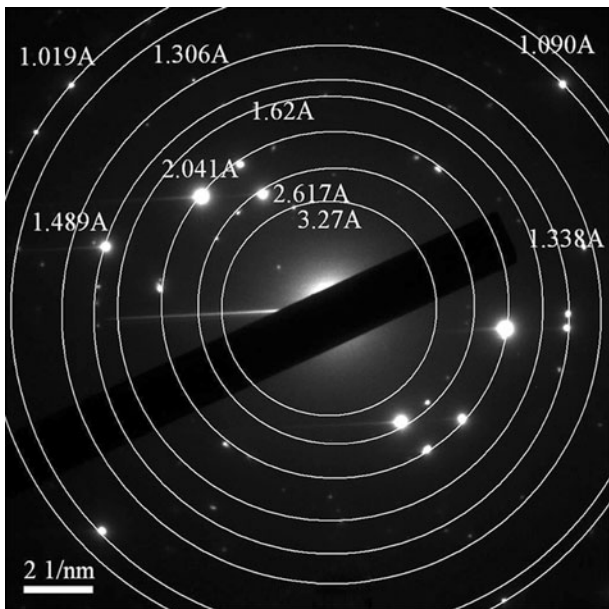

Fig. 7—Boron-aluminum interface with the reaction interlayer revealing the formation of AlB_2 and TiB_2 phases. The boron fiber was immersed for 6 h in aluminum melt containing 500 ppm Ti at 1013 K (740 °C) and rapidly withdrawn from the melt. The circled area is further examined in æ.
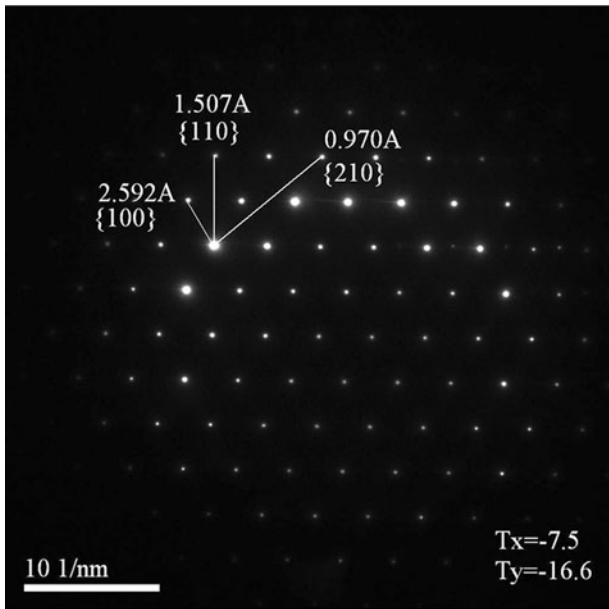
Figure 9 shows the elemental distribution of aluminum, boron, titanium and oxygen across the interface over a 2.5 μm length (c-d path in Figure 7). The boron signal has been amplified in order to reveal the details (its intensity is read on the right axis). From point c in the boron fiber, it is found that the aluminum concentration increases once the probe enters in the gray zone and then it decreases rapidly to almost zero in the TiB_2 crystal. The boron concentration, on the other hand, decreases over the gray zone, increases slightly on TiB_2 crystal and then decreases to zero in aluminum zone. It can also be noted that titanium concentration increases drastically over the blocky crystal and decreases to almost zero level over aluminum. In contrast with aluminum, there is no evidence of diffusion of Ti inside the boron filament and all titanium remains in front of the interface.

The AlB_2/TiB_2 interface was re-analyzed using a better resolution in order to enhance the oxygen concentration profile (Figure 10). The approximate zone of analysis is indicated as e-f path in Figure 7 and corresponds to the dashed rectangular zone in Figure 9. It can be seen that an oxide layer is present at the interface and acts as a marker since it does not change its position with time as compared with Figure 6. This peak is a good indicator for initial boron/melt interface.

Titanium and boron concentrations overlap over a short distance of about 50 nm and could indicate the existence of an $(Al,Ti)B_2$ phase. However, the presence of two distinct phases of TiB_2 and AlB_2 with a relatively sharp interface indicates that, at this temperature, these two phases do not form a continuous solid solution. Similar conclusions had been reported by other authors.[20,21] The Ti and boron overlap is therefore more probably an artifact due to the low spatial resolution of the EDX probe and the fact that the interface is barely parallel to the electron trajectory.
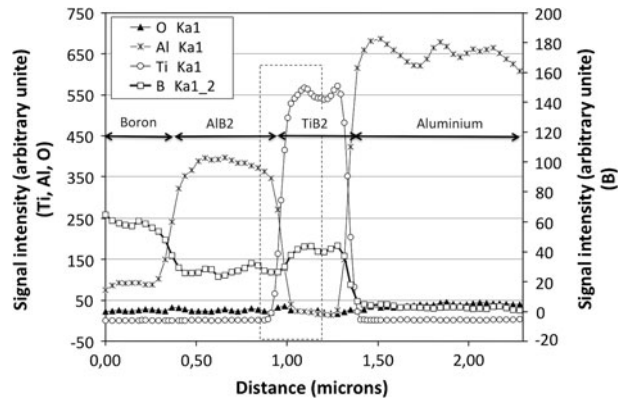
Fig. 9—Elemental linescan across the boron-aluminum interface along the c-d path shown in Fig. 7. The concentrations of aluminum, oxygen, and titanium are read on the left axis and that of boron on the right one. The arrows show four distinguished zones corresponding to different phases identified in Fig. 7.
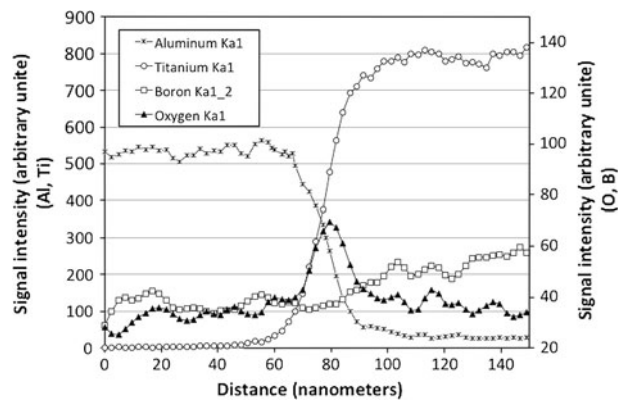

Fig. 10—Detail of the elemental composition profile at the AlB_2-TiB_2 along e-f path interface shown in Fig. 7. The concentrations of aluminum and titanium are read on the left axis and that of boron and oxygen on the right one, as indicated by arrows.

Fig. 8—Electron diffraction pattern of (a) the gray zone behind the interface corresponding to AlB_2 and (b) the blocky crystals identified as TiB_2.

It is clear that Al diffuses through the TiB_2 and oxide layers and thickens the AlB_2 zone behind the initial interface. No evidence of Al gradient within TiB_2 crystals was observed in our experiment. Since TiB_2 and $AlB2$ are not soluble in each other, the diffusion of Al through TiB_2 crystals is hardly conceivable. It is therefore logical to suppose that the diffusion of Al takes place through the TiB_2 grain boundaries. It can also be seen that the thickness of AlB_2 is not homogeneous over the examined areas. This is thus probably due to the TiB_2 grain boundary defects in some areas favoring the diffusion of aluminum (interface on the right side of Figure 7). In the same way, boron can diffuse through AlB_2 and at TiB_2 grain boundaries to reach the solid/liquid interface and react with titanium solute to thicken the TiB_2 layer. Actually the relative position of oxygen peak confirms this hypothesis since TiB_2 crystals were detected only in front of this peak.

Although these experiments revealed the mechanisms by which boron is protected in aluminum melt containing titanium, they do not clarify the grain refining mechanism of elemental boron particles as reported earlier.[19] The Al/TiB_2 interface was examined using TEM to obtain more information about the solidification of aluminum over the TiB_2 layer formed in situ. The area encircled in Figure 7 was further examined at higher magnification where a crystal of Al was found at the vicinity of a TiB_2 crystal. The inter-planar spacing of TiB_2 (001) and Al (111) planes were measured to be 0.262 and 0.230 nm, respectively. The angle between these two planes was measured to be 14.9 deg and the interface was found to be clear and free from any transitional phase. However no evidence of coherency between aluminum and TiB_2 was observed.

Examination of other TiB$_2$/Al interfaces did not reveal any coherent interface.

C. *Possible Refining Mechanism*

As mentioned earlier, the objective of this work was to understand how elemental boron particles act as an efficient grain refiner for aluminum alloys as reported by Alamdari *et al.*[19] At the light of this experiment, the refining mechanism of elemental boron seems to be close to that of Al-Ti-B master alloys and it can be attributed to the nucleation of Al directly on TiB$_2$ particles.

Grain refining mechanism of Al-Ti-B master alloys has been ardently disputed in the literature for more than 20 years. The microstructure of these master alloys consists basically of two phases within an aluminum matrix; TiB$_2$ and TiAl$_3$. The refining mechanism is therefore attributed to the nucleation of aluminum on either one of these phases. Two major hypotheses have been put forward and supported by some experimental observations to explain the refining phenomenon. The first one considers that aluminum can directly nucleate on certain crystallographic planes of a TiB$_2$ crystal while the second one only considers the nucleation of aluminum on TiAl$_3$.

Mohanthy *et al.*[12,22] showed that when Ti is absent, synthetic TiB$_2$ particles added to molten aluminum are pushed at the grain boundaries rather than being present within grains. Kaneko *et al.*[23] also reported that TiB$_2$ alone is not an efficient grain refiner.

Easton and StJohn[24] showed that TiB$_2$ are effective nucleants while the excess Ti solute restricts grain growth providing constitutional undercooling. Powerful refining effect of a master alloy, where both TiB$_2$ and Ti are present, led to development of the duplex nucleation theory. Mohanty and Gruzleski[12] detected a thin Ti-rich layer around the synthetic TiB$_2$ particles using electron probe micro analysis technique. The surrounding layer had a chemical composition close to TiAl$_3$. A crystallographic approach has also been used to explain the grain refining mechanisms. Detection of an epitaxial layer, with lattice spacing consistent with TiAl$_3$, on TiB$_2$ particles led Schumacher *et al.*[15] to conclude that such a layer could be responsible for heterogeneous nucleation of aluminum. The refining effect was thus attributed to the formation of a TiAl$_3$ layer on TiB$_2$ particles.

Low lattice disregistry between aluminum and TiAl$_3$ compared to that between aluminum and TiB$_2$[1] suggests a superior nucleation potential of the former but it does not exclude the refining potential of the latter. The interface between Al and TiB$_2$ was investigated by several authors but a consensus has not been yet reached regarding the existence of an orientation relationship between these two phases. An orientation relationship between (111) Al and (0001) TiB$_2$ planes was found in a melt-spun Al-5Ti-1B master alloy.[25] Mitra *et al.*[26] and Kostka *et al.*[27] reported semi-coherent interface between TiB$_2$ and Al where no reaction layer or segregation were found. Although these data show the good potential of certain planes of TiB$_2$ for nucleation of aluminum, the experimental conditions prevailing in these works are far from those of grain refining process. It is therefore difficult to extrapolate directly these observations to explain the grain refining process in aluminum alloys.

The interface between Al and TiB$_2$ crystals examined in the present work simulates very closely the real grain refining conditions of boron particles reported earlier.[19] A clean interface without any consistent crystallographic orientation between TiB$_2$ and Al matrix was revealed. This observation suggests that the presence of a TiAl$_3$ intermediate layer is not essential for nucleation; hence Al nucleates directly from the TiB$_2$ crystals formed *in situ* on boron particles in the melt. Consequently, in grain refining experiments with elemental boron particles, it is speculated that each boron particle acts as a substrate for nucleation of several TiB$_2$ crystallites as shown in Figures 5 and 7. These crystallites with different crystallographic orientations increase the probability of exposing a suitable TiB$_2$ facet, having minimum interface energy with α-Al, and result in higher refining efficiency of a single boron particle. It is probably the reason why elemental boron shows a higher efficiency than the conventional grain refiner with equivalent Ti and B addition levels. Another important role of TiB$_2$ crystallites is to protect boron particles and prevent their dissolution in aluminum melt.

Boron-based refiner may offer other considerable advantages compared to the conventional ones.[19] For grain refining of recycled aluminum already containing Ti, no further addition of Ti is required. In addition, no potassium fluoride salts are required in the manufacturing process, overcoming the agglomeration of TiB$_2$ particles associated with these salts. The boron particle size can be controlled during manufacturing eliminating the problems encountered with large TiB$_2$ particles. A TiB$_2$-shielded boron particle has a lower density than a bulk TiB$_2$ particle and settle less rapidly in liquid aluminum than bulky TiB$_2$ does.

IV. CONCLUSIONS

In this paper, the grain refining mechanism of boron particles was studied by observing the behavior of boron filaments immersed in Al-Ti melts in different conditions. Boron filaments were immersed into liquid aluminum having different concentrations of titanium (between 0 and 500 ppm) and the microstructure and composition at the B/Al interface were investigated. Boron filament was used to facilitate the observation of the Al-B interface.

The results showed that boron dissolves rapidly in pure aluminum. However, a concentration of about 100 ppm of Ti inhibits its dissolution. When boron comes in contact with titanium containing melts a thin layer of TiB$_2$ crystallites is formed at the surface of boron and protects it from dissolution. The boron surface is therefore covered with very fine TiB$_2$ crystals having different crystallographic orientations. The TiB$_2$ layer thickens as the boron residential time in the melt increases. Aluminum on the other hand, diffuses

through the TiB$_2$ layer and reacts with boron to form AlB$_2$ behind the TiB$_2$ layer.

During solidification, aluminum crystallizes on this *in situ* formed TiB$_2$ layer. The interface between TiB$_2$ and aluminum was found to be clean and free from TiAl$_3$ or any transitional phase. A disregistry of 15 deg was revealed between (111) Al plane and (100) TiB$_2$ plane. These observations suggest that the grain refining effect of boron is most likely due to the presence of this TiB$_2$ layer.

When a boron-based grain refiner is added to an aluminum melt, boron particles are released into the melt and a large number of TiB$_2$ crystallites with different crystallographic orientations are formed *in situ* on the surface of these boron particles. These diverse orientations increase the probability of exposing a suitable TiB$_2$ plane, (0001) planes for instance, having minimum interface energy with α-Al and result in nucleation of aluminum. This may explain why elemental boron show a higher efficiency than the conventional grain refiner with equivalent Ti and B addition levels as reported in the literature.

ACKNOWLEDGMENTS

REFERENCES

1. T.E. Quested: *Mater. Sci. Technol.*, 2004, vol. 20, pp. 1357–69.
2. A.L. Greer: *Phil. Trans. R. Soc. Lond.*, 2003, vol. A361 (1804), pp. 479–94.
3. B. Cantor: *Phil. Trans. R. Soc. Lond.,* 2003, vol. A361 (1804), pp. 409–16.
4. A.L. Greer, P.S. Cooper, M.W. Meredith, W. Schneider, P. Schumacher, J.A. Spittle, and A. Tronche: *Adv. Eng. Mater.*, 2003, vol. 5 (1–2), pp. 81–91.
5. B.S. Murty, S.A. Kori, K. Venkateswarlu, R.R. Bhat, and M. Chakraborty: *J. Mater. Process. Technol.,* 1999, vol. 90, special issue, pp. 152–58.
6. J.A. Marcantonio and L.F. Mondolfo: *Metall. Trans.*, 1971, vol. 2, pp. 465–71.
7. G.P. Jones and J. Pearson: *Metall. Trans. B*, 1976, vol. 7B, pp. 223–34.
8. P.S. Mohanty and J.E. Gruzleski: *Acta Mater.*, 1996, vol. 44 (9), pp. 3749–60.
9. K. Venkateswarlu, B.S. Murty, and M. Chakraborty: *Mater. Sci. Eng.*, 2001, vol. A301, pp. 180–86.
10. M. Johnsson: *Light Metals*, The Minerals, Metals and Materials Society, Warrendale, PA, 1992, pp. 769–77.
11. G.P. Jones: *Solidification Processing*, The Institute of Metals, Sheffield, 1987, pp. 496–99.
12. P.S. Mohanty and J.E. Gruzleski: *Acta Metall. Mater.*, 1995, vol. 43 (5), pp. 2001–12.
13. P. Schumacher and A.L. Greer: *Mater. Sci. Eng.*, 1994, vol. A178, pp. 309–13.
14. P. Schumacher and A.L. Greer: *Mater. Sci. Eng.*, 1994, vol. A181/A182, pp. 1335–39.
15. P. Schumacher, A.L. Greer, J. Worth, P.V. Evans, M.A. Kearn, P. Fisher, and A.H. Green: *Mater. Sci. Technol.*, 1998, vol. 14, pp. 394–404.
16. T. Gudmundsson, T.I. Sigfusson, D.G. McCartney, E. Wuilloud, and P. Fisher: *Light Metals*, The Minerals, Metals and Materials Society, Warrendale, PA, 1995, pp. 851–54.
17. T. Gudmundsson, G. Saevarsdottir, T.I. Sigfusson, and D.G. McCartney: *Light Metals*, Reidar Huglen, ed., The Minerals, Metals and Materials Society, Warrendale, PA, 1997, pp. 851–55.
18. K.R. Ravi, S. Manivannan, G. Phanikumar, B.S. Murty, and S. Sundarraj: *Metall. Mater. Trans. A*, 2011, vol. 42A, pp. 2028–39.
19. H. Alamdari, J. Larouche, and S. Boily: *Fonderie Fondeur d'Aujourd'hui*, 2002, vol. 217, pp. 32–42.
20. J. Fjellstedt and A.E.W. Jarfors: *Z. Metallkd*, 2001, vol. 92 (6), pp. 563–71.
21. F. Zupanic, S. Spaic, and A. Krizman: *Mater. Sci. Technol.*, 1998, vol. 14 (7), pp. 601–07.
22. P.S. Mohanty, F.H. Samuel, J.E. Gruzleski, and T.J. Kosto: *Light Metals*, U. Mannweiler, ed., The Minerals, Metals and Materials Society, Warrendale, PA, 1994, pp. 1039–45.
23. J. Kaneco, M. Sugamata, R. Shimamune, and S. Seshan: *Trans. Jpn. Foundrymen's Soc.*, 1991, vol. 10, pp. 72–75.
24. M. Easton and D. St John: *Metall. Mater. Trans. A*, 1999, vol. 30A, pp. 1625–33.
25. Y. Yang, Z. Zhang, W. Wang, and X. Bian: *Mater. Sci. Eng.*, 2004, vol. A366, pp. 17–24.
26. R. Mitra, W.A. Chiou, M.E. Fine, and J.R. Weertman: *J. Mater. Res.*, 1993, vol. 8 (9), pp. 2380–92.
27. A. Kostka, J. Lelatko, M. Gigla, H. Morawiec, and A. Janas: *Mater. Chem. Phys.*, 2003, vol. 81, pp. 323–25.